

Diffusion of Polystyrene Latex Spheres through Isotropic Rigid Rod Polymer Solutions

Douglas Gold, Clement Onyenemezu,[†] and Wilmer G. Miller*

Department of Chemistry, University of Minnesota, Minneapolis, Minnesota 55455

Received December 12, 1995; Revised Manuscript Received April 22, 1996[®]

ABSTRACT: The diffusion of highly cross-linked polystyrene latex spheres of radii 0.152 and 0.208 μm through solutions of poly(γ -benzyl-L-glutamate) (PBLG) has been studied by dynamic light scattering (DLS). The solvent used was dimethylformamide (DMF), in which PBLG adopts a rigid rodlike α -helical conformation. Tracer diffusion coefficients of the spheres in solutions of long rods ($L \approx 159$ nm) were larger than predicted from the Stokes–Einstein equation. These positive deviations from the Stokes–Einstein equation are consistent with the theory of Auvray (*J. Phys.* **1981**, 42, 79), which predicts the presence of a rod monomer depletion layer locally surrounding the spheres that extends a distance $\approx L$ from the surface of the sphere. The results are also consistent with the experimental work of others concerning depletion of stiff polymers near surfaces. Sphere tracer diffusion coefficients in solutions of smaller rods ($L \approx 48$ nm) approximately follow the Stokes–Einstein equation. In this system, depletion effects are expected to be much smaller. Fits of the sphere diffusion data to the equation $D/D_0 = \exp(-\alpha c)$ yielded values of $\nu = 1$ –1.1, which exceed those predicted by theory. We were also able to estimate translational diffusion coefficients of the PBLG in the ternary rod/sphere/solvent systems by employing very short sample times in the DLS experiment.

Introduction

Recently, research on the diffusion of highly cross-linked polystyrene (PS) latex spheres of 0.2- μm radius through solutions consisting of a random coil polymer and an organic solvent has been reported.^{1–3} Two of those studies were reported from this laboratory, in which linear polystyrene (PS)¹ and poly(methyl methacrylate) (PMMA)² were employed as matrix polymers. Concerning the linear PS/PS latex/DMF system,¹ latex sphere diffusion followed the Stokes–Einstein equation for both matrix molecular weights (2.15×10^5 and 1.1×10^6) at all matrix concentrations studied, which ranged from dilute concentrations to well beyond the matrix overlap concentration c^* . Conversely, when poly(methyl methacrylate) of molecular weight 350 000 was employed as the matrix polymer in two good solvents, positive deviations from Stokes–Einstein behavior occurred at both dilute and semidilute concentrations;² i.e., the diffusion coefficients of the latex spheres exceeded the values predicted by the Stokes–Einstein equation. It was argued that the positive deviations were caused by a layer of solution, locally surrounding the spheres, that was deficient in PMMA as compared to bulk solution, creating a local microviscosity surrounding the spheres that was lower than the bulk macroscopic viscosity. Of two possible sources of the depletion layer, namely entropic repulsion of the PMMA molecules as they approach the spheres and PS–PMMA incompatibility (immiscibility), the latter appears to be most important. This conclusion was based on the observation that depletion was absent, or at best minimal, in the aforementioned linear PS/PS latex/DMF system because the Stokes–Einstein equation was followed at all matrix concentrations studied. Since the spherical probe was chemically similar to the matrix polymer in the linear PS/PS latex/DMF system, an important aspect that made this system unique, only

entropic repulsion effects were present. These effects are apparently not important enough to cause significant depletion in the vicinity of the latex spheres.

The same PS latex spheres have been used in studying the diffusion of spheres through poly(vinyl methyl ether) ($M_w = 1.3 \times 10^6$)/toluene solutions.³ In this report, positive deviations from the Stokes–Einstein equation occurred, consistent with the assertion that the solution layer near the surface of the sphere was of lower concentration than bulk solution, i.e., depletion. Diffusion of the latex spheres was studied from dilute solution up to rather large concentrations where $c/[\eta] \approx c/c^* = 36$. Interestingly, at these high concentrations, Stokes–Einstein behavior was recovered, consistent with the theories of de Gennes which deal with polymer depletion near surfaces.^{4–6} These theories predict that the depletion layer thickness equals the matrix correlation length ξ , which decreases with matrix concentration in the semidilute regime.

The vast majority of the other experimental work concerning sphere diffusion in polymer solutions deals with non-cross-linked latex spheres diffusing through aqueous solutions of flexible or semiflexible polymers, or of coated silica spheres diffusing through solutions consisting of an organic solvent and a matrix polymer.⁷ Previously, the only reports that have appeared in the literature on sphere diffusion through rigid rod polymer solutions are those of Tracy et al.^{8,9} In those reports, the matrix polymer was poly(γ -benzyl α ,L-glutamate) (PBLG), the solvent was *N,N*-dimethylformamide (DMF), in which PBLG adopts a rigid α -helical rodlike conformation, and coated silica spheres were employed as probe particles. Three molecular weights of rod polymer, 102 000, 200 000, and 250 000, and two silica sphere radii, 39.4 and 60.4 nm, were used in the studies. In the current report, the same matrix polymer PBLG of similar molecular weights is used, and the same solvent DMF is employed. However, we have used highly cross-linked PS latex spheres of radii 152 and 208 nm as probes. Moreover, we have investigated the sphere diffusion out to higher matrix concentrations. The main experimental technique employed was dynamic light scattering (DLS).

[†] Current address: Micap Technology Corp., Niles, IL 60714.

* To whom correspondence should be addressed. FAX: 612-626-7541; e-mail: wmliller@chemsun.chem.umn.edu.

[®] Abstract published in *Advance ACS Abstracts*, July 15, 1996.

Experimental Section

Materials. Anhydrous DMF obtained from Aldrich Chemical Co. was used in all sample preparations. PBLG of two different molecular weights was obtained from Sigma Chemical Co. Values of M_w were determined by the vendor using low-angle light scattering. For the lower molecular weight PBLG, which will be referred to as PBLG70K, $M_w = 70\,000$. The higher molecular weight PBLG had $M_w = 232\,600$ and will be referred to as PBLG233K. Using a value of 1.5 \AA per residue, a weight-average length L was computed for both molecular weights. For PBLG70K, $L = 48\text{ nm}$, and for PBLG233K, $L = 159\text{ nm}$. Sigma also reported viscosity-average molecular weights of $86\,000$ and $236\,000$ for the lower and higher molecular weight PBLG samples, respectively. The PBLG was purified by reprecipitation from DMF with methanol several times and then thoroughly dried in a vacuum oven. The preparation of the highly cross-linked PS latex spheres has been described previously.^{1,10} After thorough drying, the latex spheres were dispersed in trace amounts in dry DMF by brief sonication.

PBLG solutions used in dynamic light scattering experiments were prepared by weight in dust-free cylindrical sample cells using anhydrous DMF. The specifics of sample preparation have been described previously.^{1,2} A few drops of a stock dispersion of the latex spheres in anhydrous DMF was added to the PBLG solutions so that the concentration of the spheres was $\sim 10^{-5}\text{ g/mL}$. PBLG solutions used in viscosity studies were prepared by weight with dry filtered DMF. Since PBLG is known to precipitate from DMF in the presence of trace amounts of water,¹¹ samples for all DLS and viscometry experiments were prepared in such a way as to minimize exposure to the laboratory air. After samples were prepared, they were always stored in a desiccator when not being used in an experiment.

Methods. (A) Dynamic Light Scattering. The apparatus used as the source of laser light, the detector of scattered light, and the correlator have been described previously.^{1,2} All experiments were performed in a refractive index matching fluid thermostated at $25.0 \pm 0.2\text{ }^\circ\text{C}$. DLS data were analyzed by the Laplace inversion routine CONTIN.¹² When studying the diffusion of the latex spheres, the program yielded a distribution of decay rates dominated by a single peak from which a mean decay rate was computed. Although the latex spheres dominated the scattering intensity from the PBLG/PS latex/DMF complex fluids, it was still possible to estimate the translational diffusion coefficient of the matrix PBLG by using very small sample times (10^{-6} – 10^{-5} s). In these cases, CONTIN distributions were sometimes bimodal.

(B) Viscosity. Viscosity measurements were made at $25.0 \pm 0.02\text{ }^\circ\text{C}$ using a Cannon-Ubbelohde dilution viscometer. Shear rate effects were determined using an RFS II Rheometrics rheometer.

Results

The hydrodynamic radii in DMF of the two sizes of PS latex spheres used were 152 ± 6 and $208 \pm 5\text{ nm}$. These values were determined by DLS. Electron spin resonance experiments demonstrate that these highly cross-linked latex spheres swell only minimally in DMF.¹³ Scanning electron microscopy shows that the spheres of both 152- and 208-nm radius have a narrow distribution of sizes.¹⁰ Angle-independent diffusion coefficients and single-exponential decay of the correlation function at all scattering angles indicate that no sphere aggregation occurred at the trace latex concentrations employed in this investigation.

The viscosity of PBLG70K and PBLG233K in dry DMF at $25\text{ }^\circ\text{C}$ as a function of concentration is shown in Figure 1a. It is very clear that $\partial\eta/\partial c$ is significantly larger for the PBLG233K, especially at higher concentrations. Figure 1b shows the viscosity of PBLG70K using an extended scale. The estimated mean shear rate at the capillary wall depended on PBLG concentra-

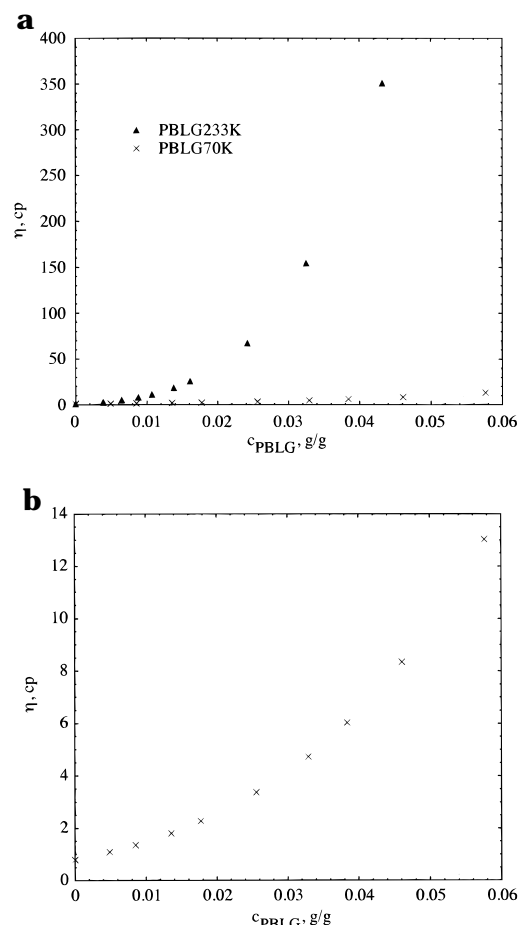


Figure 1. Concentration dependence of the zero-shear viscosity of PBLG233K and PBLG70K in dry DMF at $25\text{ }^\circ\text{C}$. In (a) viscosities of both molecular weights are shown on the same scale to highlight the large difference in $\partial\eta/\partial c$. In (b) the concentration dependence of the viscosity of PBLG70K in dry DMF at $25\text{ }^\circ\text{C}$ is displayed using a smaller scale for η .

Table 1. Specifications of Systems 1 and 2

system	sphere radius (nm)	M_w of rod	rod length (nm)	ν^a
1	152 ^b	232 600	48	1.1 ± 0.1
2	208	70 000	159	1.00 ± 0.03

^a Computed from a nonlinear least-squares fit to eq 3. ^b Values of D_{sphere} were also obtained for system 1 using a sphere of radius of 208 nm over a limited concentration range (see Figure 3).

tion and molecular weight. However, the Newtonian region extended well beyond these shear rates as evidenced by steady shear rheology measurements using a cone and plate fixture on the two most concentrated PBLG233K/DMF samples. As a result, the viscosities shown in Figure 1 may be considered to be zero shear rate values. Since diffusion measurements were performed at different matrix concentrations than the viscosity measurements, polynomial fits were made on viscosity data for interpolation.

DLS experiments were performed on two systems which are shown in Table 1. For system 1, which involves PBLG233K and PS latex spheres of radius 152 nm , DLS data concerning latex sphere diffusion were collected at 45° , 60° , 90° , and 120° . No effect of angle on the diffusion coefficient was present. Tracer diffusion coefficients of the latex spheres were determined from the slopes of Γ vs q^2 plots, where Γ is the average decay rate computed by CONTIN, and q^2 is the scattering vector. All of the Γ vs q^2 plots gave high-quality linear

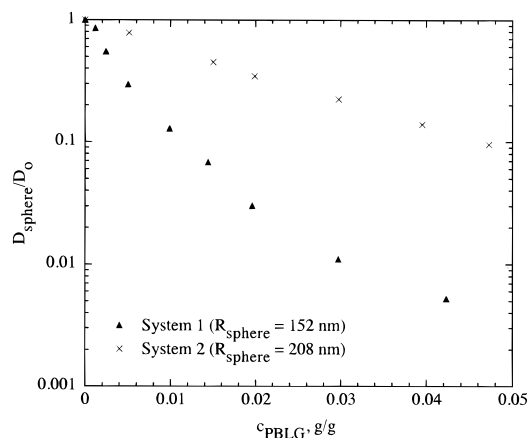


Figure 2. Plot of reduced latex sphere diffusion coefficient as a function of PBLG concentration for systems 1 and 2. For system 1, $D_0 = 1.79 \times 10^{-8} \text{ cm}^2/\text{s}$ and in system 2, $D_0 = 1.31 \times 10^{-8} \text{ cm}^2/\text{s}$.

fits with intercepts close to zero. With respect to system 2, DLS data concerning the latex spheres were taken at 45° and 60° only, after determining that the diffusion coefficients were angle-independent and that a plot of Γ vs q^2 was linear with an intercept approximately equal to zero over a range of 45–120°. Multiple runs were performed at both 45° and 60°, and little, if any, difference in values occurred. All diffusion coefficients for system 2 employed in subsequent plots are average values taken at 45°, while those for system 1 are slopes of Γ vs q^2 plots. The estimated error in the diffusion coefficients, taken as the error from linear least-squares fits for system 1, cluster around $\pm 10\%$. Similar errors are anticipated for system 2. Reduced diffusion coefficients as a function of PBLG concentration for systems 1 and 2 are displayed in Figure 2. The diffusion coefficients in both systems approach the values in the binary sphere/DMF systems. It should be noted that the majority of the data lie in the semidilute concentration regime ($c > c^*$), which begins at relatively low concentration in rigid rod polymer solutions as compared to random coil solutions. Recently, Tracy and Pecora have estimated c^* as $1/[\eta]$ for PBLG in DMF.⁸ For PBLG233K and PBLG70K in DMF, values of $c^* \approx 1/[\eta]$ were estimated to be 0.0023 and 0.015 g/g, respectively. Furthermore, the rod concentrations employed are well below those necessary for a cholesteric liquid crystalline phase to be present, so in all cases the PBLG exists in the isotropic phase.

Diffusion coefficients of spheres (D_{sphere}) in polymer solutions are often compared to those calculated from the macroscopic viscosity η through the Stokes–Einstein (SE) equation:

$$D_{\text{sphere}} = kT/6\pi\eta R \quad (1)$$

In this expression, kT is the energy term and R is the hydrodynamic radius of the spheres. If $\eta D_{\text{sphere}}/\eta_0 D_0 = 1$, where η_0 is the macroscopic zero shear rate viscosity of DMF and D_0 is the diffusion coefficient of the spheres at infinite dilution in DMF, then the SE equation is obeyed. If $\eta D_{\text{sphere}}/\eta_0 D_0 > 1$, a positive deviation from the SE equation is indicated, meaning the spheres are diffusing at a more rapid rate than given by eq 1. A negative deviation from the SE equation corresponds to $\eta D_{\text{sphere}}/\eta_0 D_0 < 1$. An alternative way of indicating behavior in the context of the SE equation is by defining a local or “microviscosity” η_μ experienced by the spheres:

$$\eta_\mu = kT/6\pi R D_{\text{sphere}} \quad (2)$$

$\eta_\mu/\eta < 1$ and $\eta_\mu/\eta > 1$ correspond to positive and negative deviations from the SE equation, respectively. Figure 3a displays a plot of $\eta D_{\text{sphere}}/\eta_0 D_0$ for systems 1 and 2. As is shown in this figure, $\eta D_{\text{sphere}}/\eta_0 D_0$ is clearly greater than unity at all matrix concentrations for system 1. In general, deviations from unity in system 1 increase with PBLG233K matrix concentration and are maximum at the largest matrix concentration studied where $\eta D_{\text{sphere}}/\eta_0 D_0 > 2$. When the molecular weight of the matrix is decreased to 70 000, system 2, deviations from unity are much less and the SE equation is obeyed within experimental error, although the mean values lie above the SE prediction. In order to show that the difference in behavior of systems 1 and 2 in the context of the SE equation is not due to the difference in sphere size, we performed a repeat experiment on system 1, using the same probe as system 2, over a limited matrix concentration range. The data are included in Figure 3a. It is clear that the behavior is similar for the two probe sizes when PBLG233K is employed as the matrix polymer. We have also elected to plot the data according to eq 2 for ease in comparison to the data reported by Tracy et al.^{8,9} This plot is shown in Figure 3b, where $\eta_\mu/\eta = \eta_0 D_0/\eta D_{\text{sphere}}$ is plotted against matrix concentration.

Phillies and co-workers^{14,15} have previously reported that probe diffusion D in the presence of matrix polymer often follows a “stretched exponential” relationship:

$$D/D_0 = \exp(-\alpha c^v) \quad (3)$$

where D_0 is the sphere diffusion coefficient in the absence of matrix polymer, c is the matrix concentration, α is a constant for a given matrix molecular weight and probe size, and v is a scaling parameter. Nonlinear least-squares analysis yields values of the scaling parameter v for systems 1 and 2, which appear in Table 1.

Discussion

Test of the Stokes–Einstein Equation. In general, Figures 3a and 3b demonstrate that the latex spheres immersed in a matrix of shorter rods ($L \approx 48$ nm) obey the SE equation within experimental error at the PBLG concentrations studied, while the spheres in a matrix of longer rods ($L \approx 159$ nm) exhibit significant positive deviations from the SE equation. Moreover, the origin of this difference of behavior in the context of the SE equation can be traced to rod length, as opposed to sphere size. This is also demonstrated in Figure 3 in that the positive deviations in system 1 persist when the same spherical probe used in system 2 is employed. Consequently, the data suggest that if the rod length is short enough, the spheres will follow the SE equation; conversely, large rods result in sphere diffusion that deviate in a positive sense from the SE equation.

Our experimental data agree with the theoretical predictions of Auvray,¹⁶ who derived the rod monomer concentration profile for hard rods of length L and diameter d ($L \gg d$) in a solvent near a planar surface. This theory was based on steric rod–rod and rod–plane interactions. Auvray’s model predicts a layer of solution near the planar surface of depleted rod monomer concentration as compared to bulk solution. This depletion layer forms because of a reduction of configurational entropy as a rod approaches the planar surface. Rodlike

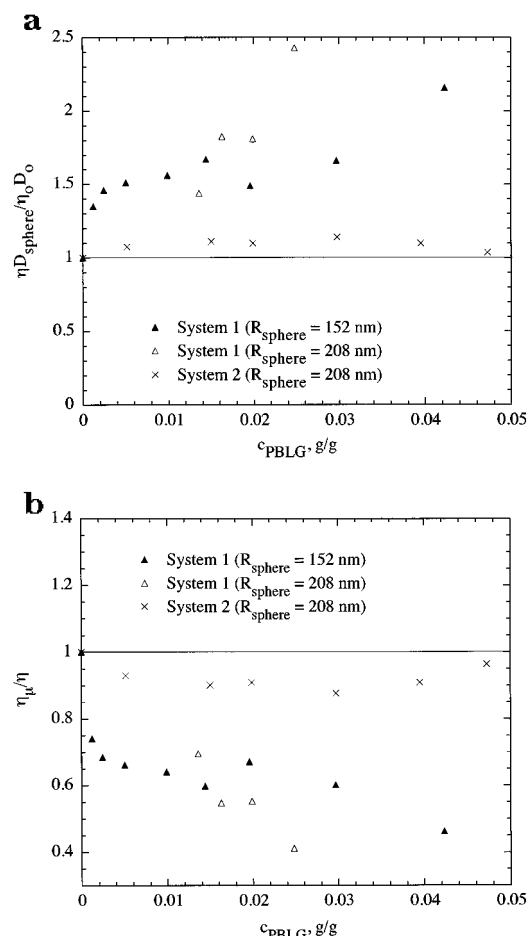


Figure 3. Test of the Stokes–Einstein equation as a function of PBLG concentration for systems 1 and 2: (a) $\eta D_{\text{sphere}}/\eta_0 D_0$ vs PBLG concentration; (b) η_{μ}/η vs PBLG concentration. Solid lines are expected values for SE behavior.

molecules have configurational entropy because of molecular rotation. As a rod approaches the planar barrier, some of those rotational configurations are excluded, creating an “entropic repulsion” between the rod and the plane which is only dependent on L . The result is a depletion layer that, in the case of Auvray’s derivation, has a thickness $\delta \approx L$. Beyond a distance L from the planar surface, bulk rod monomer concentration is recovered. Some interesting features of Auvray’s model are that the derived concentration profile expression can be applied to both dilute and semidilute rod concentrations up to the liquid crystal transition and that $\delta \approx L$ is not concentration dependent throughout both the dilute and semidilute rod concentration regimes. Auvray’s derived expression for the monomer concentration profile for a rod near a planar surface is

$$\begin{aligned} c(z) &= c_b(z/L)(1 - \ln(z/L)) & \text{for } z < L \\ &= c_b & \text{for } z > L \end{aligned} \quad (4)$$

where z is the distance from the plane. Auvray also derived the monomer concentration profile for hard rods near hard spheres for a ternary solution of hard rods, hard spheres, and a solvent.¹⁶ The derivation was conducted in a similar fashion as the rod/solvent/plane problem previously discussed. Indeed, the expression for the concentration profile reduces to eq 4 when a/L is very large, where a is the radius of the sphere. Three concentration regions (I, II, and III) emerged from Auvray’s theory for rod depletion around spheres.

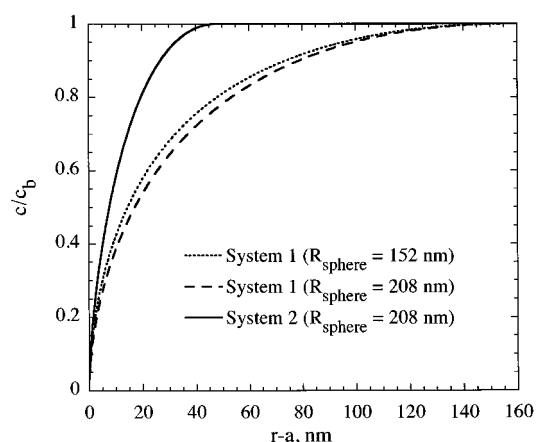


Figure 4. Rod monomer concentration relative to bulk concentration c/c_b vs radial distance from surface of sphere, $r - a$, for systems 1 and 2. The plots are based on Auvray’s model for the rod monomer concentration at a point r from the center of a sphere of radius a .

Regions I and II extend from the surface of the sphere radially out to a distance equal to the rod length. In these two regions the rod monomer concentration is less than the bulk concentration c_b because of a reduction of configurational entropy. Beyond a distance L from the surface of the sphere, region III, bulk rod monomer concentration is recovered. Auvray’s derived expression for the rod monomer concentration profile near a sphere of radius a at a radial distance r from the center of the sphere is somewhat complicated. It is eq 3 in Auvray’s paper. We have used this equation to plot the rod monomer concentration profiles, which appear in Figure 4, for our two rod/sphere/solvent systems. In this figure, we plot the rod monomer concentration relative to bulk concentration c/c_b vs distance from the surface of the sphere $r - a$.

If a rod depletion zone is locally surrounding the spheres in our systems, as is predicted by Auvray’s model, the microviscosity experienced by the spheres η_{μ} would be less than the bulk macroscopic viscosity. Indeed, $\eta_{\mu} < \eta$ for system 1, as shown in Figure 3b. In general, the magnitudes of the deviations from unity for system 1 increase with PBLG concentration, becoming maximum at the largest matrix concentration studied where $\eta D_{\text{sphere}}/\eta_0 D_0 \approx 2.2$ and $\eta_{\mu}/\eta \approx 0.45$ for a probe radius of 152 nm. This can be reconciled with Auvray’s model, since it predicts that δ remains constant with increasing PBLG concentration, while $\partial\eta/\partial c$ increases quite rapidly with PBLG233K concentration, as shown in Figure 1a. Consequently, one might expect magnitudes of deviations to increase with matrix concentration. It is possible that the depletion layer thickness δ actually decreases past c^* , as is anticipated for flexible^{4–6} and semiflexible^{17,18} polymers near surfaces. Indeed, experiments using stiff polymers near planar surfaces¹⁸ and spheres¹⁹ have demonstrated that δ decreases in the semidilute regime. However, if the increase in $\partial\eta/\partial c$ outweighs any decrease in δ , one would still expect magnitudes of SE deviations to increase with concentration.

Figure 3 demonstrates that the shorter rods of system 2 show only small, if any, deviation from the SE equation at the matrix concentrations studied. This is likely due to three factors. First, $\delta \approx L$ is only 48 nm for system 2 as compared to 159 nm for system 1. Consequently, since the depletion layer thickness is much smaller for system 2, it should have a smaller

effect on the SE deviations. Second, according to Figure 4, for a given distance $r - a$ from the surface of the sphere that lies in the depletion layer, the relative rod monomer concentration (c/c_b) is greater for system 2, which again diminishes the effect of depletion as compared to system 1. Third, as is evident from Figure 1, $\partial\eta/\partial c$ is much smaller for the rods of $L \approx 48$ nm (PBLG70K) in DMF than rods of $L \approx 159$ nm (PBLG233K) in DMF. This will also tend to diminish the effect of rod depletion on SE deviations. The combined effects of the three aforementioned factors apparently cause SE deviations for shorter rods to be minimal, if present at all. The small apparent positive deviations in this system could be due to small depletion effects that one might anticipate in this system.

It may seem a bit risky to apply Auvray's model for depletion layers near surfaces, which has been derived for static equilibrium situations, to our systems which involve diffusion. In Auvray's derivation, the spherical barriers are considered stationary, while only the rods can move. However, the self-diffusion coefficient of the spheres is 1–3 orders of magnitude smaller than the self-diffusion coefficient of the rods (D_{self} for the PBLG rods will appear in an upcoming paper). Consequently, in our systems, a sphere is diffusing at a much slower rate than the rods and may be approximated as a stationary entity. As a sphere slowly moves from an initial point, the rods can rapidly relocate, creating a new depletion layer. We suggest that this process is continuous as the sphere diffuses throughout the solution.

It may also seem risky to apply Auvray's model to the PBLG/PS latex/DMF system because it only takes into account steric rod–sphere interactions. Any specific interactions between the PBLG rods and the PS latex spheres unrelated to rotational configurational entropy are not incorporated into the model. However, the fact that system 2, which involves the shorter rods, essentially follows the SE equation is compelling evidence that no strong repulsive enthalpic interactions exist between the spheres and rods. If such strong interactions were present, this system would be expected to exhibit strong positive deviations from the SE equation as well. Consequently, at least as a first approximation, we feel Auvray's model is an appropriate one for our rod/sphere/solvent systems.

Other experimental evidence supports our contention of the presence of depletion layers in systems involving rodlike or semiflexible polymers near surfaces. Ausserre, Hervet, and Rondelez studied the interfacial depletion layer between an aqueous solution of xanthan, a stiff polysaccharide, and a planar silica surface using an evanescent-wave-induced fluorescence technique.²⁰ The xanthan had a molecular weight of 1.8×10^6 and a radius of gyration of 159 nm, and gave rise to a depletion layer of thickness 150 nm in dilute solution. The data in dilute solution agreed with both a model for semiflexible chains and Auvray's model for fully rigid rods near a planar barrier. In a subsequent report,¹⁸ the same authors investigated the concentration dependence of the depletion layer thickness for xanthan near a planar barrier. The depletion layer thickness remained constant at about 150 nm in dilute xanthan solutions but decreased with concentration in semidilute solutions. Since only the model for semiflexible chains was compatible with the concentration dependence of the mean depletion layer thickness in semidilute solution, this model was deemed most appropriate. Au-

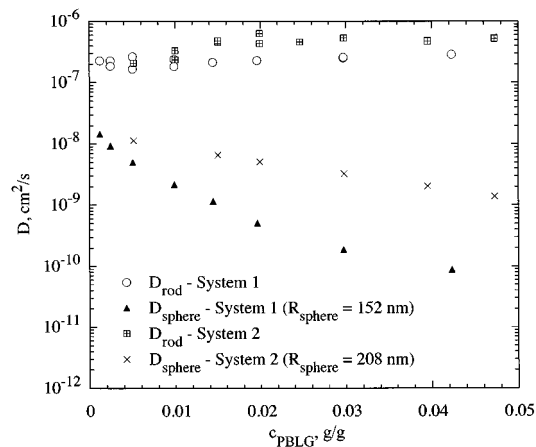


Figure 5. Plot of the PBLG translational diffusion coefficient (D_{rod}) as a function of concentration for systems 1 and 2. Latex sphere tracer diffusion coefficients (D_{sphere}) are shown for comparison.

vray's model for rods near a planar surface predicts a depletion layer of thickness L at all dilute and semidilute concentrations. Cosgrove, Obey, and Ryan used nuclear magnetic resonance to estimate the depletion layer thickness for poly(styrenesulfonate) (PSS) in silica dispersions.¹⁹ Depletion layer thicknesses of over 85 nm surrounding the silica particles were reported for PSS of molecular weight 780 000, the largest of four molecular weights used in the report. Depletion layer thicknesses were found to decrease with increasing PSS concentration. Finally, flocculation of colloidal particles upon the addition of a flexible or semiflexible polymer has been attributed to polymer depletion layers surrounding the colloidal particles.^{21–32} Other examples of depletion layers have been discussed in two review articles.^{33,34}

PBLG Translational Diffusion. By employing very short sample times at large scattering angles (90° and 120°) in the DLS experiment, we were able to probe sources of relatively fast fluctuations of the scattered light intensity. Using sample times $\sim 10^{-6}$ s in the DLS experiments involving the rod/sphere/solvent samples, as opposed to sample times of 10^{-4} – 10^{-2} s used to study sphere diffusion, resulted in CONTIN distributions that contained a single dominant mode. Although the spheres dominate the light scattering intensity, employing these short time windows causes the scattering from the spheres to lack the fluctuations necessary for autocorrelation by the correlator. Consequently, faster processes within the system, such as the translational diffusion of PBLG, can be probed. For the PBLG70K/sphere/DMF system (system 2), the dominant slower mode in the CONTIN distribution of decay rates was assigned to the translational diffusion of the PBLG, as has been done by others.⁸ A weak faster mode, which may be due to rod translation–rotation coupling,⁸ was sometimes present in addition to the dominant mode. Regarding the PBLG233K/sphere/DMF system (system 1), the dominant CONTIN mode was also assigned to translational rod diffusion. As the rod concentration was decreased in system 1, a significant slow mode attributable to sphere tracer diffusion began to grow in the CONTIN distribution. A plot of the diffusivities extracted from the modes assigned to translational rod diffusion in both systems vs rod concentration appears in Figure 5; sphere tracer diffusion coefficients from both systems are shown for comparison. It should be kept in mind that a large amount of "noise" from the

scattering of the spheres was present when the data concerning rod translational diffusion were acquired. Consequently, the modes were often broad, and the diffusivities extracted from them should be viewed as approximate. Nevertheless, the diffusivities extracted from the modes associated with translational PBLG diffusion are generally consistent with those reported for similar molecular weights of PBLG in binary PBLG/DMF solutions.^{35–38} Moreover, as one would expect, the trace amount of spheres dispersed in our systems does not significantly affect the PBLG translational diffusion when compared to PBLG translational diffusion in binary rod/solvent systems. Tracy and Pecora came to the same conclusion for their PBLG ($M_w = 102\,000$)/silica sphere/DMF system.⁸

Two important aspects of Figure 5 should be noted. First, the initial small rise in D_{rod} for system 2 may be due to the onset of semidilute rod dynamics, since it occurs around $c^* \approx 1/[\eta] \approx 0.015$ g/g in this system. A similar observation was reported by Tracy and Pecora for translational diffusion of PBLG ($M_w = 102\,000$) in DMF as c^* was approached.⁸ In that report, an analogous increase in D_{rod} occurred at c^* in both a binary rod/solvent system and a ternary rod/sphere/solvent system. Second, the rod translational diffusion coefficient is much less sensitive to rod concentration changes than sphere diffusion. In order to appreciate this observation, one must realize that all the diffusion coefficients that are represented in Figure 5 are *mutual* diffusion coefficients which contain both thermodynamic and hydrodynamic contributions. With respect to the translational diffusion of the rods, the repulsive thermodynamic interactions between rods tend to cause the mutual diffusion coefficient to increase with rod concentration.³⁵ However, hydrodynamic effects in the form of enhanced friction tend to cause the mutual diffusion coefficient to decrease with rod concentration.³⁵ Consequently, the ongoing competition between thermodynamic and hydrodynamic factors has the effect of making the rod translational diffusion coefficient relatively insensitive to rod concentration. The latex spheres, on the other hand, are present in trace amounts so the mutual diffusion coefficient approaches the self-diffusion or tracer diffusion coefficient of the spheres, which contains no thermodynamic component. Hence, the increased friction with increasing rod concentration causes the sphere diffusion coefficient to decrease strongly with rod concentration, especially for system 1 involving PBLG233K.

Comparison with the Work of Tracy et al. The data reported by Tracy et al.^{8,9} concerning the diffusion of coated silica spheres through PBLG/DMF solutions are in general agreement with our data. Solutions of longer rods ($L = 137$ and 171 nm) yielded positive deviations from the SE equation for silica spheres of radii 39.4 and 60.4 nm, and silica spheres of radius 60.4 nm in solutions of shorter rods ($L = 70$ nm) followed the SE equation. For solutions of PBLG of length 137 nm (mol wt = 200 000), magnitudes of deviations from the SE equation were similar for both sphere sizes. In these systems the maximum deviations occurred at the largest matrix concentrations studied (0.0105–0.0130 g/mL), where $\eta_r/\eta \approx 0.8$ for both sphere sizes. For PBLG of length 171 nm (mol wt = 249 700), a sphere radius of 60.4 nm yielded a maximum deviation in η_r/η of ≈ 0.8 , which occurred at the largest matrix concentration studied of 0.0131 g/mL. However, the smaller probe of radius 39.4 nm yielded a maximum deviation in η_r/η of

≈ 0.5 , which occurred at a rod concentration of 0.004 g/mL, followed by a trend back toward unity, and then another drop so that $\eta_r/\eta \approx 0.6$ at the highest matrix concentrations studied (0.0131 g/mL). The effect of sphere size was somewhat unclear based on their data. It is clear that our data broadly agree with the data of Tracy et al. in that longer rods yield positive deviations from the SE equation for sphere diffusion, while shorter rods result in adherence to the SE equation.

The interpretation we have offered, concerning a rod depletion layer surrounding the spheres, is quite different from that offered by Tracy et al. They proposed that a pre-nematic change in the PBLG/sphere/DMF solution structure occurs at higher PBLG concentrations, which causes the positive deviations from the SE equation. This interpretation was somewhat supported by total intensity light scattering experiments. They determined that it was unlikely that the change in solution structure was due to polymer-induced phase separation but rather was possibly related to nonuniformities that have been observed in macroscopic pulp fiber suspensions,³⁹ which form flocs. However, we observed no evidence of PBLG flocs as our CONTIN distributions contained no very slow mode that would likely result. Tracy et al. reported that they observed no slow mode either, but suggested that the flocs may be undetectable by the DLS experiment if they do not persist for a long enough period of time. Consequently, the interpretation proposed by Tracy et al. is certainly possible. However, we do believe one should be very cautious when comparing PBLG solutions to pulp fiber suspensions, as the former constitutes a single-phase system while the latter a two-phase system. Consequently, the systems are likely quite different from a thermodynamic point of view.

Scaling Behavior. Theories that model sphere diffusion through rod/solvent systems predict a dependence of D on rod concentration of the form of eq 3. In 1973, Ogston et al. used a stochastic model to describe sphere diffusion through a random distribution of long rigid molecular fibers.⁴⁰ The model predicts that $\nu = 0.5$. Cukier, in 1984, also predicted $\nu = 0.5$ based on his model for the diffusion of dilute Brownian spheres in a semidilute solution of rodlike polymers.⁴¹ Our experimentally determined value of ν is 1–1.1 (Table 1), which is somewhat larger than the value reported by Tracy and Pecora⁸ of 0.81 for silica spheres in solutions of PBLG of molecular weight 102 000. To date, these are the only experimental values of ν available for sphere diffusion through a rigid rod matrix. Evidently, the available theoretical models underestimate ν and do not satisfactorily describe spherical particle diffusion in these systems.

Conclusion

We have studied the diffusion of highly cross-linked PS latex spheres through rigid rod polymer solutions. Our results are consistent with the model of Auvray,¹⁶ which predicts a rod monomer depletion layer locally surrounding the spheres. This interpretation is in agreement with our results of sphere diffusion through random coil matrix solutions in which positive deviations from the Stokes–Einstein equation were attributed to polymer depletion near the spheres.² Our data are broadly consistent with the work of Tracy, Garcia, and Pecora;^{8,9} however, we have offered a different interpretation. It is clear that more work needs to be performed on similar systems in order to

clearly understand the microstructure of rod/sphere/solvent systems. To this end, we are currently attempting to probe polymer depletion layers in these systems.

Acknowledgment. This work was supported in part by the Graduate School, University of Minnesota, by the National Science Foundation through the Center for Interfacial Engineering, and by the Stanwood Johnston Memorial Fellowship (D.G.).

References and Notes

- (1) Onyenezu, C. N.; Gold, D.; Roman, M.; Miller, W. G. *Macromolecules* **1993**, *26*, 3833.
- (2) Gold, D.; Onyenezu, C. N.; Miller, W. G. *Macromolecules* **1996**, *29*, 5700.
- (3) Won, J.; Onyenezu, C.; Miller, W. G.; Lodge, T. P. *Macromolecules* **1994**, *27*, 7389.
- (4) de Gennes, P.-G. *Scaling Concepts in Polymer Physics*; Cornell University Press: London, 1979.
- (5) de Gennes, P.-G. *Macromolecules* **1981**, *14*, 1637.
- (6) Joanny, J. F.; Leibler, L.; de Gennes, P.-G. *J. Polym. Sci., Polym. Phys. Ed.* **1979**, *17*, 1073.
- (7) For example, see refs 1–18 and 21–25 of the previous paper of this issue.
- (8) Tracy, M. A.; Pecora, R. *Macromolecules* **1992**, *25*, 337.
- (9) Tracy, M. A.; Garcia, J. L.; Pecora, R. *Macromolecules* **1993**, *26*, 1862.
- (10) Onyenezu, C. Ph.D. Thesis, University of Minnesota, 1994.
- (11) Russo, P. D. Ph.D. Thesis, University of Minnesota, 1981.
- (12) Provencher, S. W. *Makromol. Chem.* **1979**, *180*, 201.
- (13) Fedie, R. L.; Miller, W. G. *Polym. Mater. Sci. Eng.* **1994**, *71*, 344.
- (14) Phillies, G. D. J.; Malone, C.; Ullmann, K.; Ullmann, G. S.; Rollings, J.; Yu, L.-P. *Macromolecules* **1987**, *20*, 2280.
- (15) Phillies, G. D. J.; Ullmann, G. S.; Ullmann, K. *J. Chem. Phys.* **1985**, *82*, 5242.
- (16) Auvray, L. *J. Phys.* **1981**, *42*, 79.
- (17) Ausserre, D.; Hervet, H.; Rondelez, F. *J. Phys. Lett.* **1985**, *46*, L-929.
- (18) Ausserre, D.; Hervet, H.; Rondelez, F. *Macromolecules* **1986**, *19*, 85.
- (19) Cosgrove, T.; Obey, T. M.; Ryan, K. *Colloids Surf.* **1992**, *65*, 1.
- (20) Ausserre, D.; Hervet, H.; Rondelez, F. *Phys. Rev. Lett.* **1985**, *54*, 1948.
- (21) Sperry, P. R.; Hopfenberg, H. B.; Thomas, N. L. *J. Colloid Interface Sci.* **1981**, *82*, 62.
- (22) Feigin, R. I.; Napper, D. H. *J. Colloid Interface Sci.* **1980**, *75*, 525.
- (23) De Hek, H.; Vrij, A. *J. Colloid Interface Sci.* **1981**, *84*, 409.
- (24) Gast, A. P.; Hall, C. K.; Russel, W. B. *J. Colloid Interface Sci.* **1983**, *96*, 251.
- (25) Goddard, E. D.; Vincent, B., Eds. *Polymer Adsorption and Dispersion Stability*; ACS Symposium Series 240; American Chemical Society: Washington, DC, 1984; Chapter 16.
- (26) Gast, A. P.; Hall, C. K.; Russel, W. B. *Faraday Discuss. Chem. Soc.* **1983**, *76*, 189.
- (27) Sperry, P. R. *J. Colloid Interface Sci.* **1984**, *99*, 97.
- (28) Gast, A. P.; Russel, W. B.; Hall, C. K. *J. Colloid Interface Sci.* **1986**, *109*, 161.
- (29) Vincent, B.; Edwards, J.; Emmet, S.; Jones, A. *Colloids Surf.* **1986**, *18*, 261.
- (30) Vincent, B.; Edwards, J.; Emmet, S.; Croot, R. *Colloids Surf.* **1988**, *31*, 267.
- (31) Fleer, G. J.; Scheutjens, J. M. H. M.; Cohen Stuart, M. A. *Colloids Surf.* **1988**, *31*, 1.
- (32) Dubin, P. L.; Tong, P., Eds. *Colloid–Polymer Interactions*; ACS Symposium Series 532; American Chemical Society: Washington, DC, 1993; Chapter 13.
- (33) Rondelez, F.; Ausserre, D.; Hervet, H. *Annu. Rev. Phys. Chem.* **1987**, *38*, 317.
- (34) Fleer, G. J.; Cohen Stuart, M. A.; Scheutjens, J. H. H. M.; Cosgrove, T.; Vincent, B. *Polymers at Interfaces*; Chapman and Hall: London, 1993.
- (35) Russo, P. S.; Karasz, F. E. *J. Chem. Phys.* **1984**, *80*, 5312.
- (36) Delong, L. M.; Russo, P. S. *Macromolecules* **1991**, *24*, 6139.
- (37) Kubota, K.; Chu, B. *Biopolymers* **1983**, *22*, 1461.
- (38) Kubota, K.; Tominaga, Y.; Fujime, S. *Macromolecules* **1986**, *19*, 1604.
- (39) Kerekes, R. J.; Schell, C. J. *J. Pulp Pap. Sci.* **1992**, *18*, 32.
- (40) Ogston, A. G.; Preston, B. N.; Wells, J. D. *Proc. R. Soc. London A* **1973**, *333*, 297.
- (41) Cukier, R. I. *Macromolecules* **1984**, *17*, 252.

MA951823P